

This is the peer reviewed version of the following article: Podolski-Renić A, Bősze S, Dinić J, Kocsis L, Hudecz F, Csámpai A, Pešić M. Ferrocene–cinchona hybrids with triazolyl-chalcone linkers act as pro-oxidants and sensitize human cancer cell lines to paclitaxel. *Metalomics*. 2017;9(8):1132–41.
<http://dx.doi.org/10.1039/C7MT00183E>



© The Royal Society of Chemistry 2017

Ferrocene - Cinchona Hybrids with Triazolyl - chalcone Linker Act as Pro-oxidants and Sensitize Human Cancer Cell Lines to Paclitaxel

Ana Podolski-Renić,^a Szilvia Bősze,^b Jelena Dinić,^a László Kocsis,^c Ferenc Hudecz,^{b,c} Antal Csámpai,^d and Milica Pešić^{a*}

^a*Department of Neurobiology, Institute for Biological Research “Siniša Stanković” (IBISS), University of Belgrade, Belgrade, Serbia. Email: camala@ibiss.bg.ac.rs*

^b*MTA-ELTE Research Group of Peptide Chemistry, Eötvös Loránd University, Budapest, Hungary*

^c*Department of Organic Chemistry, Eötvös Loránd University (ELTE), Budapest, Hungary*

^d*Department of Inorganic Chemistry, Eötvös Loránd University (ELTE), Budapest, Hungary*

* Corresponding author

Abstract

Recently, we demonstrated that ferrocene- containing compounds with cinchona moiety displayed marked anticancer activity. Here we report on the effects of most promising isomers encompassing quinine- (compounds **4** and **5**) and quinidine - epimers (compounds **6** and **7**) - synthesized by improved methods providing controlled diastereoselectivity - in three different human multidrug resistant (MDR) cancer cell lines and their sensitive counterparts (non-small cell lung carcinoma NCI-H460/R/NCI-H460, colorectal carcinoma DLD1-TxR/DLD1 and glioblastoma U87-TxR/U87). We observed that the presence of MDR phenotype did not diminish the activity of compounds suggesting that ferrocene quinine- and quinidine - epimers are not substrates for P-glycoprotein which was indicated as a major mechanism of MDR in cell lines used. Considering that metal-based anticancer agents could mainly act by increasing ROS production, we investigated the potential of ferrocene-quinidine epimers to generate ROS. We found that **6** and **7** more readily increased ROS production and induced mitochondrial damage in MDR cancer cells. According to cell death analysis, **6** and **7** were more active against MDR cancer cells showing collateral sensitivity. In addition, our data suggest that these compounds could act as inhibitors of autophagy. Importantly, simultaneous treatments of **6** and **7** with paclitaxel (PTX) increased sensitivity of MDR cancer cells to PTX. In conclusion, the ferrocene - quinidine epimers besides being selective towards MDR cancer cells could also possess potential to overcome PTX resistance.

Introduction

Multidrug resistance (MDR) as a major obstacle to efficient cancer treatment is described by the simultaneous resistance to diverse drugs that could be structurally and functionally unrelated. Various molecular mechanisms are involved in MDR, including reduced drug accumulation due to overexpression of membrane transporters, altered drug targets, diminished response to apoptotic signalling and enhanced drug detoxification.¹ Since MDR is one of the main reasons for cancer treatment failure, finding new agents able to eliminate MDR cancer cells is a research priority for successful therapy outcome.

Metal-based agents are commonly used in cancer therapy.^{2, 3} Besides classical metal-complexes containing halide-, oxygen- and nitrogen-donor ligands there is a wide variety of organic cytostatic agents with or without metal component. Among organometallics, ferrocene derivatives with diverse molecular architectures are of pronounced importance. A concept taken into account for the design of such potential therapeutic agents was that replacement of an aromatic nucleus of certain organic compounds for a ferrocene unit with tuneable redox character can lead to products possessing unexpected properties which are absent or less manifested in the parent molecule.^{4, 5} There are also remarkable examples of active metallocene derivatives comprising chalcone moiety.

For instance, ferrocenylprop-2-en-1-ones were demonstrated to strongly inhibit the HepG2 cells while having no toxicity towards healthy human fibroblasts.⁶ On the other hand, it is well-documented that the application of quinine derivatives in the field of cancer diagnosis⁷ and in chemotherapy^{8, 9} goes far back to the past. Our previous results have shown that cinchona-ferrocene conjugates with amide and urea spacers display significant *in vitro* activity against MCF-7 breast adenocarcinoma, HepG2 hepatoma, HL-60 leukaemia and SH-SY5Y neuroblastoma human cell lines.¹⁰ Besides this acylation-based approach, in cinchona chemistry utilizing click strategy have a real potential in searching for novel lead structures as demonstrated by the significant *in vitro* antiproliferative effects of hybrids with 1,4-disubstituted 1,2,3-triazole linker containing nucleoside⁹ or polyether residue.¹¹ In this line our previous study showed that ferrocene-cinchona hybrids tethered *via* chalcone- and 1,2,3-triazole moieties exhibit pronounced *in vitro* cytostatic effect on HEPG2 and HT-29 cell lines.¹²

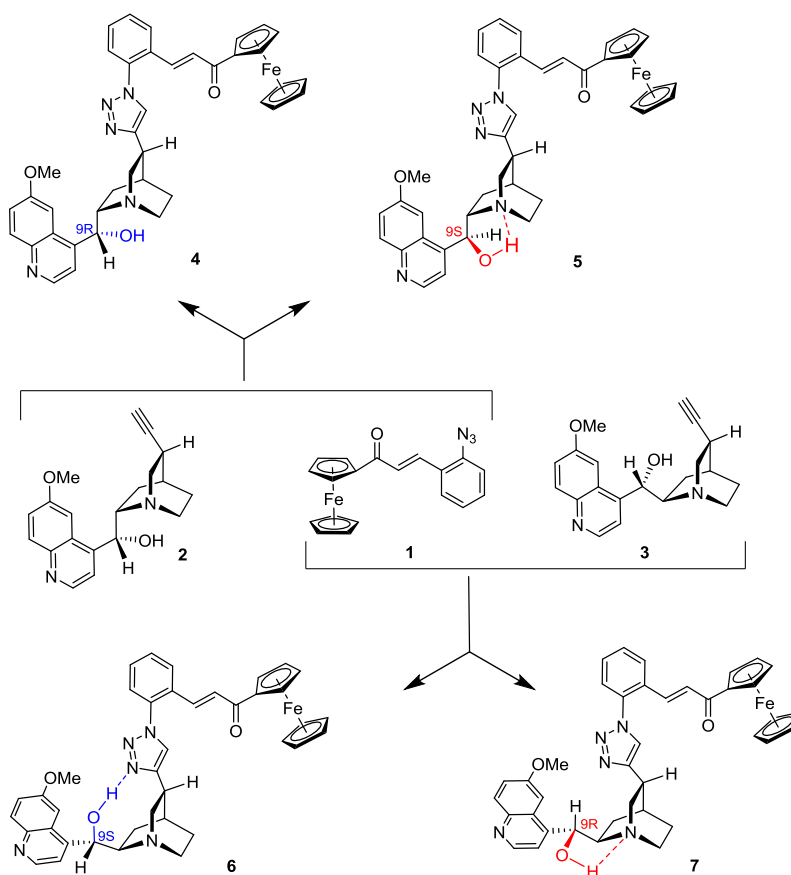
In this work, four isomers encompassing ferrocene-quinine (compounds **4** and **5**) and -quinidine epimers (compounds **6** and **7**) were resynthesized with the intention of avoiding C9-epimerization to provide controlled access to products with retained relative configuration of the cinchona fragment (Scheme 1). The anticancer activity of the four diastereoisomers was tested in three pairs of sensitive and MDR cancer cell lines developed by adaptation to paclitaxel (PTX) and doxorubicin (DOX).^{13, 14} Besides cytotoxic activity, the impacts of **6** and **7** on reactive oxygen and nitrogen species (ROS and RNS) production, cell death and on autophagy modulation were investigated. In addition, the potential of **6** and **7** to sensitize MDR cancer cells towards PTX was also assessed.

Results and discussion

Chemistry

The copper(I)-mediated azide-alkyne click reactions of azide **1** and cinchona-based epimeric alkynes **2** and **3**, respectively, conducted under standard conditions afforded hardly separable mixtures of the epimeric products (cf. Methods i. and ii. in Table 1).¹² In order to avoid the use of demanding separation techniques and to improve isolated yields, we envisaged to elaborate improved procedures to enable diastereoselective formation of C9-epimeric pairs **4/5** and **6/7**. Thus, these compounds were

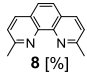
expected to become easily accessible models for extensive biological assays, which might disclose correlations between activity and relative configuration with pronounced relevance in binding to biological targets. It is assumed that the partial epimerization of C9 stereogenic centre in the cinchona residue takes place via reversible deprotonation enabled by the coordination of Cu(I)-species to quinoline N1-atom.¹² Accordingly, the use of an increased catalyst loading (Method iii.: Table 1) led to the formation of epiquinine and epiquinidine derivatives **5** and **7** which were isolated as single products in high yields (87% and 72%, resp.). When the click reactions were conducted in the presence of neocuproine **8** as a chelating ligand (Method iv. in Table 1), capable of sequestering copper ions, diastereomers **4** and **6** with retained quinidine scaffold were isolated as single products in low yields (27% and 23%, respectively) pointing to a partial copper-deactivation. On the other hand, in both cases prolonged reaction times led to increased conversions at the expense of diastereoselectivity (Method v.: Table 1). We also observed that higher loading of **8** partly deactivates the catalyst system as suggested by the isolated yields (Method vi.: Table 1).



Reaction conditions and the yields of the products are listed in Table 1

Scheme 1: Synthesis of epimeric ferrocene-cinchona hybrids with triazolyl-chalcone linkers

Table 1. Conditions and the yields of the epimeric pairs of products of the copper-catalyzed click reactions $1 + 2 \rightarrow 4 + 5$ and $1 + 3 \rightarrow 6 + 7$, respectively (Scheme 1).

Method	Reaction conditions ^a employing <i>n</i> -BuOH / H ₂ O (1:1) as solvent				Yields of the products [%]			
	CuSO ₄ ·5H ₂ O [%]	Na-ascorbate [%]	 8 [%]	Reaction time [h]	4	5	6	7
i.)	1	5	0	10	23	51	21	39
ii.)	4	20	0	2	12	82	15	54
iii.)	10	50	0	6	0	87	0	72
iv.)	2	10	2	6	27	0	23	0
v.)	2	10	2	24	29	10	32	9
vi.)	2	10	4	6	12	0	7	0

^a The reactions were conducted at 25 °C.

Sensitivity of cancer cells to ferrocene-cinchona alkaloids

The promising IC₅₀ values of ferrocene-cinchona conjugates on different cancer cell lines¹² inspired us to evaluate newly synthesized ferrocene-quinine and -quinidine epimers for their capacity to inhibit the cell growth of three corresponding sensitive/MDR cancer cell line pairs. Since we assumed that the relative configuration of the tested compounds might significantly control the binding to the biological targets, two stereoisomer pairs were synthesized under improved reaction conditions capable to control the relative configuration of the products. Although the efficacy of ferrocene-quinine and -quinidine epimers varied among different cancer cell lines, the majority of IC₅₀ values were below 10 μM indicating high anticancer potential of tested compounds (Table 2). Ferrocene-quinidine epimers **6** and **7** showed better selectivity pattern towards MDR cancer cells than ferrocene-quinine epimers (**4** and **5**). Sensitivity of U87-TxR cells to all tested ferrocene-quinine and -quinidine epimers was higher in comparison with their sensitive counterparts, U87 cells. Even more, ferrocene-quinidine epimer **7** showed significant selectivity towards two MDR cancer cell lines, DLD1-TxR and U87-TxR with more than 2 fold lower IC₅₀ values than those obtained in corresponding sensitive cell lines. Although compound **6** showed the best inhibitory effect in all six cancer cell lines, with IC₅₀ values varying between 1.6 and 3.0 μM, according to SRB assay, this compound showed slight selectivity only towards U87-TxR. Therefore, based on inhibitory potential and selectivity towards MDR cells, ferrocene-quinidine epimers (**6** and **7**) were chosen for further studies using two pairs of sensitive and MDR cancer cell lines (DLD1/DLD1-TxR and U87/U87-TxR).

Table 2. Sensitivity of non - MDR and MDR cancer cells to ferrocene-quinine and -quinidine epimers (expressed as IC₅₀ ± SD values in μM)

compound	4	5	6	7
DLD1	5.83 ± 0.05	7.50 ± 0.04	1.75 ± 0.08	10.71 ± 0.02
DLD1-TxR	3.89 ± 0.02	10.14 ± 0.06	1.60 ± 0.08	4.43 ± 0.06
U87	5.36 ± 0.08	6.30 ± 0.07	3.00 ± 0.08	6.25 ± 0.06
U87-TxR	4.59 ± 0.04	3.13 ± 0.06	2.31 ± 0.07	2.30 ± 0.02
NCI-H460	6.15 ± 0.09	6.79 ± 0.08	2.34 ± 0.02	4.00 ± 0.07
NCI-H460/R	4.85 ± 0.06	6.04 ± 0.04	2.13 ± 0.03	3.65 ± 0.04

The efficiency of anticancer drugs is often limited by appearance of MDR. Quite opposite, the effects of tested compounds were not diminished by the presence of MDR. Moreover, compound **7** exerted significant growth inhibitory effects against DLD1-TxR and U87-TxR cells, showing collateral sensitivity (CS). CS is described as a phenomenon when MDR cells became more sensitive to a certain drug than their corresponding sensitive cells.¹⁵ Several mechanisms have been proposed to account for CS. One of them is the ability of CS agents to modify intracellular redox status, yielding the production of reactive oxygen species (ROS).¹⁶ CS agents could generate ROS in both MDR and sensitive cancer cells, but in some cases, increased vulnerability of MDR cells to ROS was observed.¹⁷

Pro-oxidative effects of ferrocene-quinidine epimers

In recent years, several studies indicated that ferrocene complexes increase ROS production in cancer cells and such complexes have become an increasingly popular motif in the development of cancer therapeutics.^{18, 19} Therefore, the potential of ferrocene-quinidine epimers to generate free radicals were examined by dihydroethidium (DHE)/ dihydrorhodamine 123 (DHR) staining. Superoxide anion, hydrogen peroxide (ROS) and peroxy nitrite anion (RNS) generation were detected in sensitive and MDR cells after 48 h exposure to **6** and **7** (Figure 1A, B).

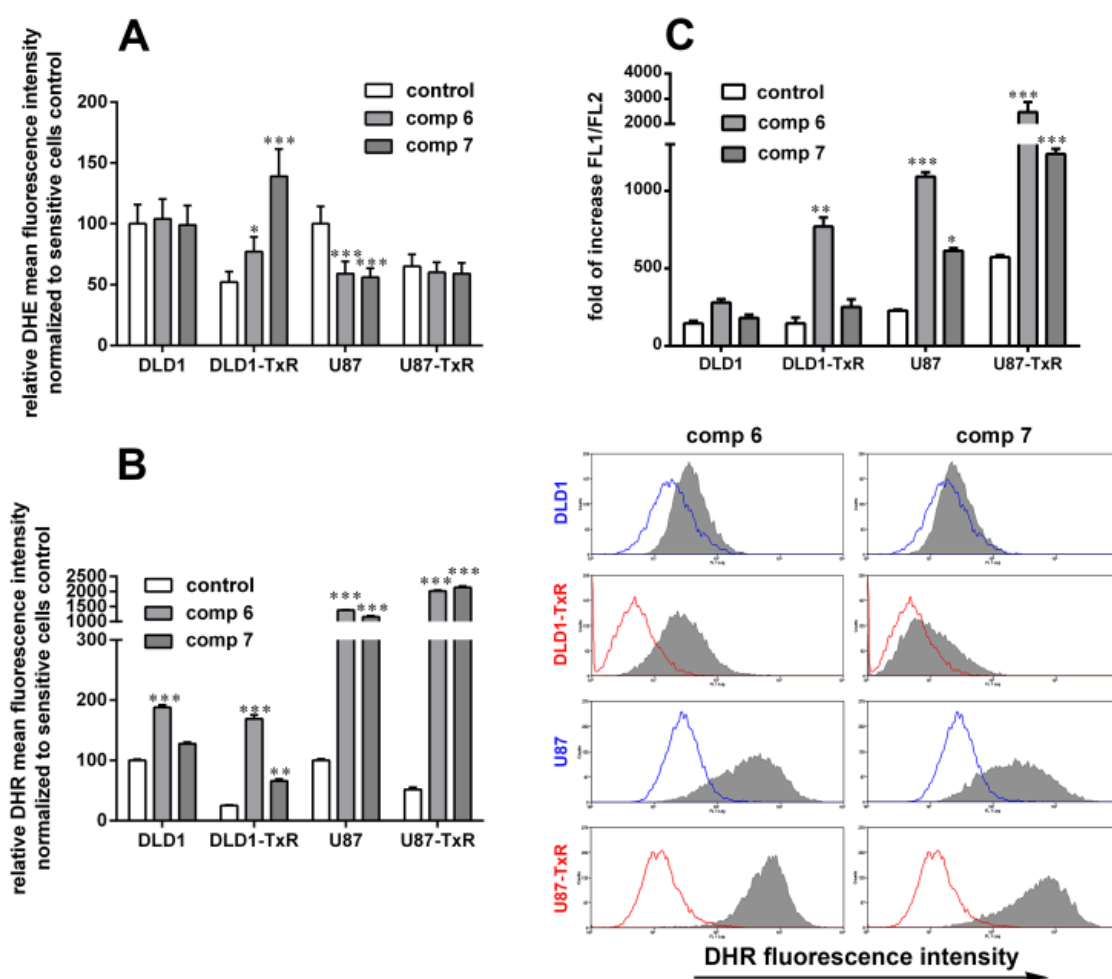


Figure 1. Changes in ROS production and mitochondrial membrane potential induced by ferrocene-quinidine epimers. Detection of ROS production levels by (A) DHE and (B) DHR labelling (right panel with representative flow cytometric profiles) in colorectal carcinoma cells (DLD1 and DLD1-TxR) and glioblastoma cells (U87 and U87-TxR) treated with **6** and **7** for 48 h. (C) An increase in the ratio of green to red fluorescence (FL1/FL2) assessed by JC-1 staining (described in the Experimental section) in DLD1 and DLD1-TxR cells as well as U87 and U87-TxR cells treated with **6** and **7** for 48 h. The experiments were performed three times (n = 3). Statistically significant difference compared to corresponding untreated controls: p < 0.05 (*), p < 0.01 (**), p < 0.001 (***)

Treatments with **6** and **7** induced significant increase in DHE intensity in DLD1-TxR cells (1.5-fold and 2.7-fold, respectively), while the effect in DLD1 cells was neglectable (Figure 1A). Compounds **6** and **7** decreased DHE fluorescence intensity in U87 cells while superoxide anion production upon **6** and **7** treatments was not changed in U87-TxR cells (Figure 1A). Intensity of DHR fluorescence after treatments with **6** and **7** significantly increased in both cell lines (Figure 1B). Other authors showed the early increase in the ROS production when cancer cells were exposed to compounds with ferrocene moiety for only 10 min.²⁰ Therefore, it is reasonable to think that the extreme elevation in the hydrogen peroxide (ROS) and peroxynitrite anion (RNS) content after 48 h of incubation with our compounds is the consequence of the early impact of ferrocene on ROS production. Namely, the superoxide anion production (detected by DHE) paves the way and contributes to hydrogen peroxide (ROS) and peroxynitrite anion (RNS) production (detected by DHR). Pro-oxidative effect of ferrocene-quinidine epimers was more pronounced in both MDR colorectal carcinoma (DLD1-TxR) and MDR glioblastoma (U87-TxR) cells (Figure 1B).

Earlier, we showed that glioblastoma MDR cells have lower antioxidant capacity than their corresponding sensitive counterpart.^{13, 17} Herein we confirmed that the basal level of ROS and RNS was significantly decreased in both MDR cancer cell lines compared to their sensitive counterparts (Figure 1A, B), while ROS and RNS production was more pronounced in both MDR cell lines after application of **6** and **7** (Figure 1B). One key feature of ferrocene is that it can undergo a one electron oxidation, yielding the ferrocenium cation ($\text{Fc}^{2+} / \text{Fc}^{3+}$). This redox reaction is reversible for most ferrocene derivatives.²¹ Study reported by Mooney et al. also showed that ferrocene derivatives may generate hydroxyl radicals from hydrogen peroxide.²² Therefore, capability of **6** and **7** to modulate redox status could be the reason for their selective activity against MDR cancer cells. It is known that production of free radicals is tightly regulated by the intrinsic antioxidant defence systems. Previous studies have suggested that impaired antioxidant defence could affect the sensitivity of MDR cells to pro-oxidants.^{17, 23} It is likely that vulnerability to ferrocene-quinidine epimers also lays in lower anti-oxidative capacity of two MDR cancer cell lines.

Since increase in ROS and RNS production mostly affects mitochondrial function,²⁴ we studied the ability of **6** and **7** to change mitochondrial membrane potential in MDR and sensitive cells by using JC-1 labelling (Figure 1C). Compound **6** induced prominent depolarization of mitochondrial membrane in all cancer cell lines, while less notable effect was observed only in DLD1 cells (Figure 1C). Compound **7** depolarized mitochondrial transmembrane potential in both glioblastoma cell lines, while exerting more significant effect in U87-TxR cells (Figure 1C).

Our results showed that ROS and RNS production induced by compound **6** was accompanied by depolarization of mitochondrial transmembrane potential in both sensitive and MDR cancer cells. However, loss of mitochondrial membrane potential was more prominent in MDR cancer cell which is in accordance with the stronger pro-oxidative potential of this compound in MDR cells. Compound **7** depolarized mitochondrial transmembrane potential only in glioblastoma cells in which, it increased ROS and RNS production more profoundly than in colorectal carcinoma cells. Thus, we assume that

mitochondria of MDR cancer cells are more susceptible to oxidative stress caused by **6** and **7**. The mitochondrial inner membrane is vital for ATP generation through the mitochondrial respiratory chain. Depolarization of mitochondrial membrane potential leads to blockade of the respiratory chain, which results in decreased efficiency of ATP production.²⁵ Intracellular ATP levels have a role in the interplay between apoptosis and necrosis and depletion of intracellular ATP level leads to the activation of cell death pathways.²⁶ Since increased ROS production alters the mitochondrial membrane potential and damages the respiratory chain,²⁷ it eventually initiates cell death. Therefore, next we analysed the cell death induction after treatments with **6** and **7**.

The effects of ferrocene-quinidine epimers on cancer cell death and autophagy

One of the vital cellular processes that mitochondria regulate is apoptosis.²⁸ As response to pro-apoptotic stimuli, such as ROS production, mitochondrial membrane potential decreases. This leads to the release of cytochrome c from the mitochondria and the subsequent assembly of the apoptosome complex that is required for the activating of downstream effector caspases.²⁹ In order to investigate whether loss of mitochondrial membrane potential induced by ferrocene-quinidine epimers initiates cell death, sensitive and MDR cancer cells treated with **6** and **7** were subjected to Annexin-V-FITC (AV)/Propidium Iodide (PI) staining. The effects were assessed after 48 h. Both ferrocene-quinidine epimers significantly increased a portion of late apoptotic and necrotic, but not early apoptotic cells in colorectal carcinoma cell lines (Figure 2). The effects of both compounds were more pronounced in DLD1-TxR cells. Glioblastoma cell lines were less sensitive to cell death induction than colorectal carcinoma cell lines (Figure 2). We observed significant increase in the percentage of glioblastoma cells in early and late apoptosis as well as in necrosis after exposure to **6** and **7** (Figure 2). Both compounds, but particularly **6**, were more efficient in MDR glioblastoma cells (Figure 2). Apoptosis and necrosis are considered as two major types of cell death. However, autophagy, which is primarily recognized as cytoprotective process, has been involved in both types of cell death.²⁶

Autophagy is a multi-step process in which macromolecules and damaged organelles are recycled in order to maintain cellular homeostasis. This process involves the engulfment of cytoplasmic material and intracellular organelles into autophagosomes, which is followed by fusion with a lysosome where the captured material is degraded.³⁰ Key proteins involved in autophagy pathway are ubiquitin-like protein microtubule-associated protein-1 light chain 3 (LC3) and polyubiquitin-binding protein (p62/SQSTM1).³¹ During autophagosome formation a key feature is the conversion of cytosolic form LC3-I to the membrane bound form, LC3-II. This protein remains on mature autophagosomes until fusion with lysosomes, and it is commonly used as a marker for autophagy.³²

Another common autophagic marker is p62, a protein that binds directly to the autophagy effectors LC3-I and LC3-II. Since p62 itself is degraded during autophagy, a correlation between inhibition of autophagy and increased levels of p62 has been proposed.^{33, 34} In order to explore potential of ferrocene-quinidine epimers to modulate autophagy, we assessed the amount and cellular distribution of the autophagosomal marker LC3 as well as the amount of autophagy flux marker p62 (Figure 3).

Both compounds increased LC3 expression level in DLD1-TxR cells in which, CQ exerted the strongest effect (Figure 3A). They also increased p62 expression level similarly to CQ implying that they could act through the same way as autophagy inhibitor CQ (Figure 3B). The highest increase in accumulated p62 was observed in MDR colorectal carcinoma cells after treatment with compound **6** (Figure 3B). Autophagic vesicles labelled with anti-LC3 antibody were visualized in sensitive and MDR cancer cells after 48 h treatment with **6**, **7** and CQ (Figure 3C). Treatment with autophagy inhibitor CQ, which prevents the autophagosome/lysosome fusion, caused excessive cytoplasmic

accumulation of LC3 puncta. Both ferrocene-quinidine epimers inhibited autophagy pathway which resulted in the appearance of LC3 puncta in the cytoplasm (Figure 3C). Again, more pronounced effect was observed after treatment with compound 6 (Figure 3C).

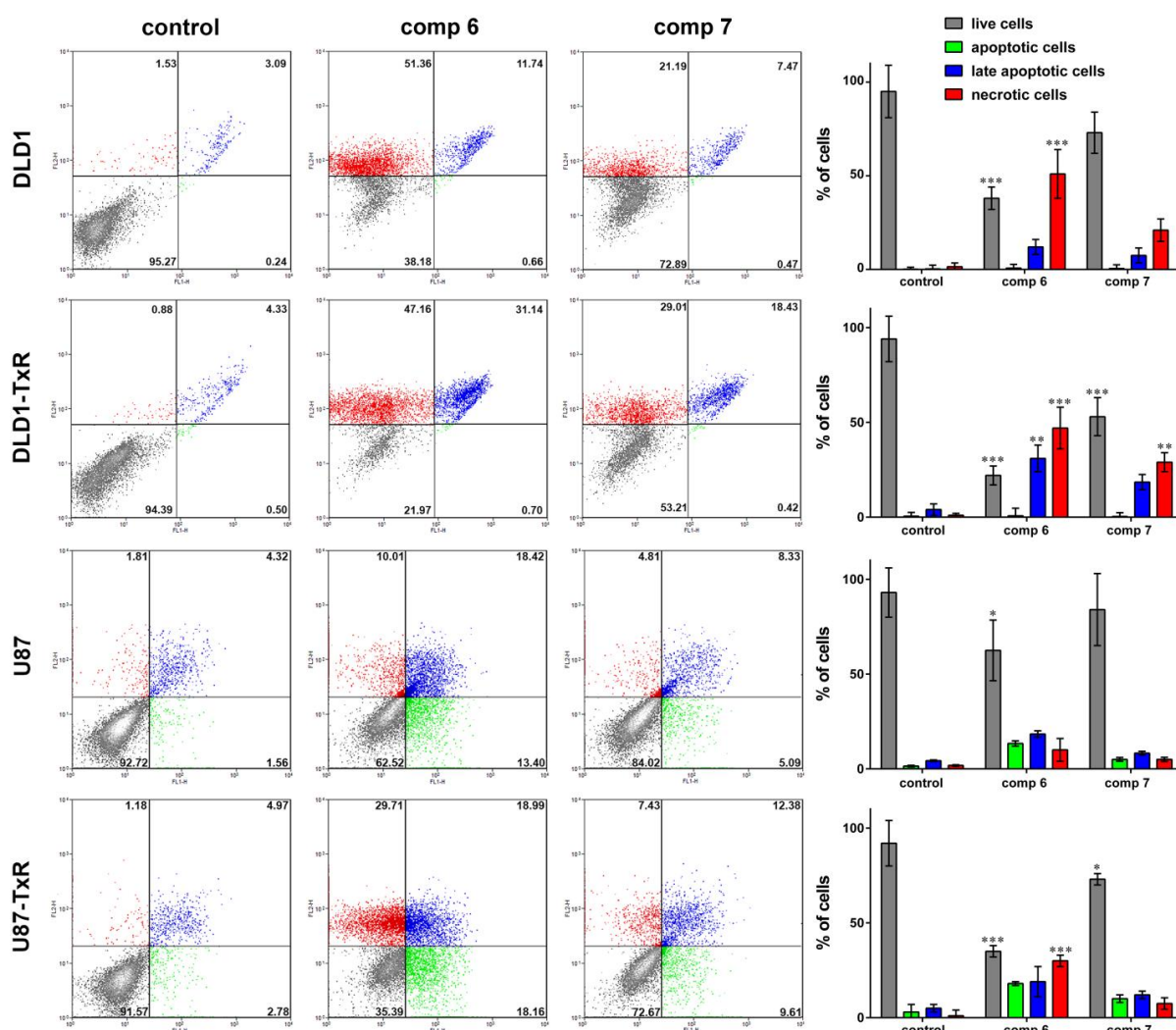


Figure 2. Cell death induction by ferrocene-quinidine epimers. Cell death was assessed by AV/PI staining after 48 h. Flow cytometric assay distinguishes viable (black: AV- PI-), early apoptotic (green: AV+ PI-), late apoptotic (blue: AV+ PI+) and necrotic (red: AV- PI+) cells. The experiments were performed three times (n = 3). Representative two dimensional dot-plots are shown followed by quantification and statistical analysis on the right panel. Statistically significant difference compared to corresponding untreated controls: p < 0.05 (*), p < 0.01 (**), p < 0.001 (***).

Autophagy is a defence mechanism of the cell which enables cells survival during stresses such as hypoxia, nutrient deprivation and ROS production.³⁵ In addition to its cytoprotective function, autophagy can also promote cell death.^{26, 32} Therefore, the relationship between autophagy and apoptosis has been extensively investigated. Crosstalk between autophagy and apoptosis exists at many levels since these pathways share molecular components involved in the regulation of both processes. Recent studies indicated that association between autophagy and apoptosis is mediated by

p62.³² This autophagy flux marker interacts with caspase-8 and enables its aggregation and activation thus initiating apoptotic pathway.³⁶ Moreover, it is known that ROS production have an important role in the induction of autophagy.³⁷ However, Ci et al., has recently found that ROS inhibited autophagy by downregulating the expression of protein required for autophagy induction ULK1 in human acute promyelocytic leukaemia cell line.³⁸ Hence, we assume that ferrocene-quinidine epimers inhibit autophagy by increasing ROS production. Increased ROS levels induce accumulation of p62 which in turn initiates apoptosis. On the other hand, the suppression of autophagy may lead to the accumulation of dysfunctional mitochondria with increased production of ROS.

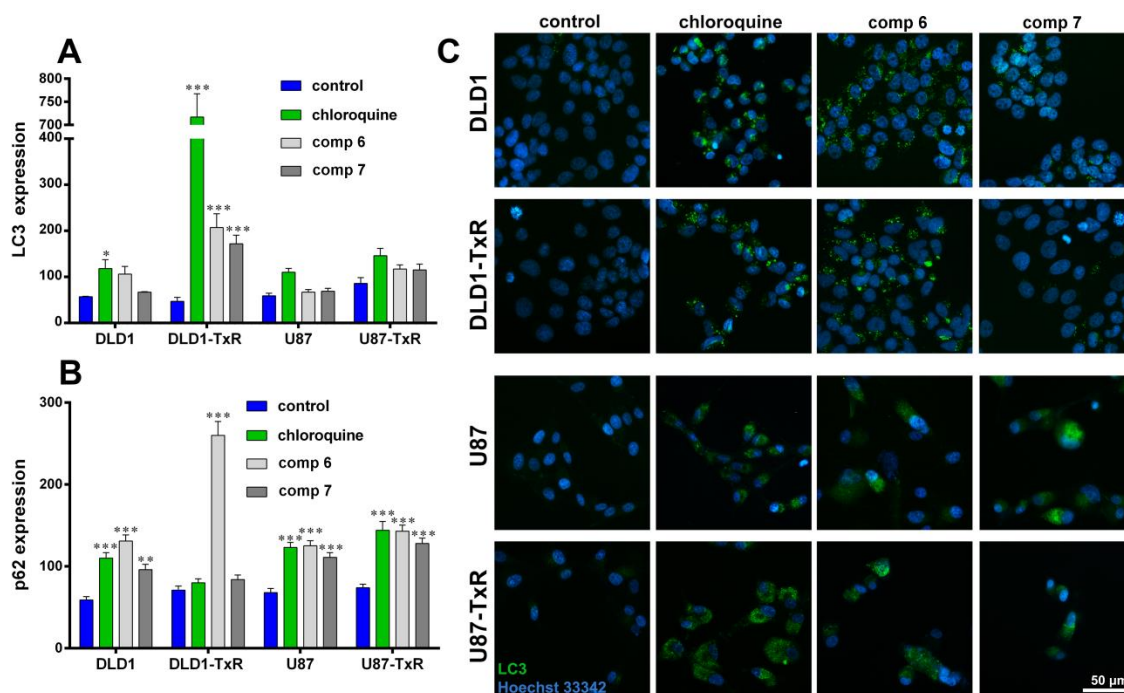


Figure 3. Modulation of autophagy by ferrocene-quinidine epimers. (A) Changes in the expression level of LC3 detected by flow cytometry in DLD1, DLD1-TxR, U87 and U87-TxR cells after 48 h treatment with **6**, **7** and CQ. (B) Changes in the expression level of p62 detected by flow cytometry in DLD1, DLD1-TxR, U87 and U87-TxR cells after 48 h treatment with **6**, **7** and CQ. (C) Accumulation of autophagosomes (green) in the cytoplasm after 48 h treatment with **6**, **7** and CQ visualized according to the anti-LC3 antibody labelling. Nuclei were counterstained with Hoechst 33342 (blue). Scale bar = 50 μm.

Enhancement of PTX sensitivity by ferrocene-quinidine epimers

To investigate whether ferrocene-quinidine epimers could increase the sensitivity of MDR cancer cell lines to PTX, we examined their interaction with PTX in simultaneous combinations (Table 3, Figure 4). We showed earlier that both MDR cancer cell lines are resistant to PTX.¹³ Compounds **6** and **7** significantly enhanced the growth inhibitory effect of PTX (Figure 4A). Moreover, ferrocene-quinidine epimers decreased the IC₅₀ values for PTX in a concentration- dependent manner showing stronger efficacy in DLD1-TxR cells (Table 3). There was no difference in the potential of **6** and **7** to sensitize MDR cells to PTX (Table 3). We subjected these results to computerized synergism/antagonism CalcuSyn software analysis. The majority of examined combinations between

ferrocene-quinidine epimers and PTX demonstrated additive (CI values close to 1) or synergistic (CI < 1) interactions (Figure 4B). The observed synergy was higher in DLD1-TxR cells (Figure 4B).

Table 3. Relative reversal of PTX resistance by quinidine epimers in MDR cancer cells

Compounds	concentration (nM)	DLD1-TxR	Relative reversal*	U87-TxR	Relative reversal*
		IC ₅₀ _{PTX} ± SD (nM)		IC ₅₀ _{PTX} ± SD (nM)	
PTX	concentration (nM)	367.19±6.01		1447.80±75.69	
6	250	190.61±4.81	1.93	776.03±55.93	1.87
	500	167.65±5.83	2.19	664.16±49.66	2.18
	1000	73.43±5.11	5.00	442.06±39.47	3.27
7	500	227.56±5.96	1.61	780.20±57.77	1.86
	1000	150.11±5.09	2.45	660.69±51.21	2.19
	2500	53.74±4.77	6.83	385.89±29.56	3.75

*Relative reversal of PTX resistance expressed as the ratio of IC₅₀ values between PTX alone and PTX combined with quinidine epimers

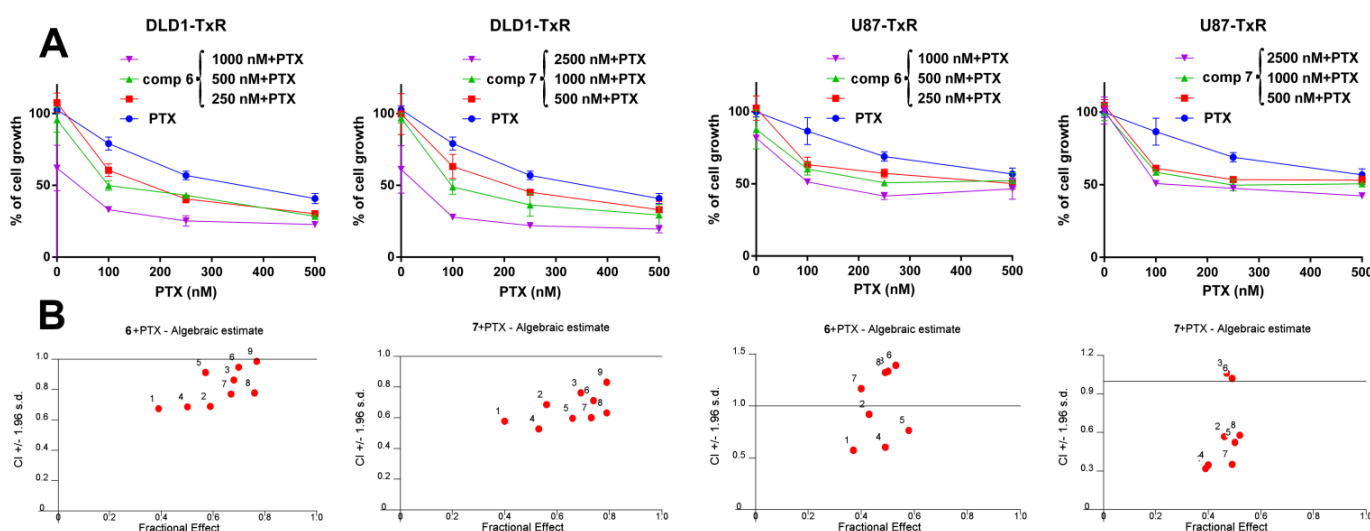


Figure 4. Ferrocene-quinidine epimers enhance the sensitivity of MDR cancer cells to PTX. (A) The effects of simultaneous combinations of **6** and **7** with PTX on DLD1-TxR and U87-TxR cell growth were assessed by SRB assays. Average ± S.D. values were calculated from three independent experiments (n = 3). (B) The interactions between ferrocene-quinidine epimers and PTX were analysed by CalcuSyn software. Values of CI < 1 point to synergistic effect, while CI close to 1 indicates an additive effect.

Experimental

Chemicals

All chemicals and solvents for syntheses were obtained from commercially available sources (Aldrich, Fluka) and used without further purification. Merck Kieselgel (230–400 mesh, 60 Å) was used for flash column chromatography.

RPMI 1640 medium, Minimum Essential Medium (MEM), fetal bovine serum (FBS), antibiotic-antimycotic solution, penicilin-streptomycin solution, L-glutamine and trypsin/EDTA were purchased from Bioind, Beit Haemek, Israel. Sulforhodamine B (SRB), dimethyl sulfoxide (DMSO) and chloroquine (CQ) were obtained from Sigma-Aldrich Chemie GmbH, Germany. Annexin-V-FITC (AV) apoptosis detection kit with Propidium Iodide (PI) was purchased from Abcam, Cambridge, UK. Dihydroethidium (DHE) and dihydrorhodamine 123 (DHR) were obtained from Molecular Probes®, Invitrogen, USA, while JC-1 kit was purchased from BD Biosciences, San Diego, USA. Anti-LC3A/B antibody and secondary antibody Alexa Fluor 488 goat anti-rabbit IgG (H+L) were purchased from Cell Signaling Technology®, USA, while rabbit p62 antibody was obtained from Novus Biologicals, USA.

Drugs

Compounds **4**, **5**, **6** and **7** were first synthesized by Methods i.) and ii.) as published before.¹² PTX was purchased from Sigma-Aldrich Chemie GmbH, Germany. Compounds **4**, **5**, **6** and **7** were diluted in DMSO and 20 mM aliquots were kept at 4 °C. PTX was diluted in absolute ethanol and 1 mM aliquots were stored at -20°C. Before treatment, all drugs were freshly diluted in sterile water.

Copper-catalyzed click reactions affording compounds 4, 5, 6 and 7 with controlled diastereoselectivity (Methods iii.)-vi.)

Method iii.): Azido component **1** (357 mg, 1 mmol), the cinchona-based alkyne (2 or 3: 323 mg, 1 mmol), CuSO₄·5H₂O (25 mg, 0.1 mmol) and sodium ascorbate (99 mg, 0.5 mmol) were stirred under argon in a mixture of n-BuOH (3 mL) and H₂O (3 mL) for 6 h at room temperature and the resulted suspension was diluted with water (50 mL). The obtained precipitate was filtered off and subjected to column chromatography on silica employing first CH₂Cl₂/MeOH (100/1) as eluent to recover a small amount of unreacted **1** (10-15 mg). Subsequent elution with CH₂Cl₂/MeOH (50:1) afforded the corresponding quinidine-based triazole hybrid (5: 591 mg, 87% or 7: 489 mg, 72%) which was crystallized with MeOH/H₂O (1/3).

Methods iv.)-vi.): Azido component **1** (357 mg, 1 mmol), the cinchona-based alkyne (2 or 3: 323 mg, 1 mmol), CuSO₄·5H₂O (5 mg, 0.02 mmol) and sodium ascorbate (20 mg, 0.1 mmol) and ligand **8** [4.2 mg, 0.02 mmol (iv. and v.); 8.2 mg, 0.04 mmol (vi.)] were stirred under argon in a mixture of n-BuOH (3 mL) and H₂O (3 mL) [for 6 h (iv. and vi.); for 24 h (v.)] at room temperature and the resulted suspension was diluted with water (50 mL). The obtained precipitate was filtered off and subjected to column chromatography on silica employing first CH₂Cl₂/MeOH (100/1) as eluent to recover unreacted **1** (205-280 mg). Subsequent elution with CH₂Cl₂/MeOH (50:1) afforded triazoles [4: 183 mg, 27% (iv.), 197 mg, 29% (v.), 81 mg, 12% (vi.); 5: 0% (iv., vi.), 68 mg, 10% (v.); 6: 156 mg, 23% (iv.), 217 mg, 32% (v.), 48 mg, 7% (vi.); 7: 0% (iv., vi.), 61 mg, 9% (v.)] which were crystallized with MeOH/H₂O (1/3). The analytical and spectral data of products **4-7** were practically identical to those reported in Kocsis et al.¹²

Cell culture

DLD1 (human colorectal carcinoma, DLD-1 is one of two colorectal adenocarcinoma cell lines which were isolated by D.L. Dexter and associates during a period from 1977-1979) and U87 (human glioblastoma, U-87 MG abbreviation for Uppsala 87 Malignant Glioma) and NCI-H460 (human non-small cell lung carcinoma, the NCI-H460 cell line was derived by A.F. Gazdar and associates in 1982 from the pleural fluid of a patient with large cell cancer of the lung) cell lines were purchased from the American Type Culture Collection, Rockville, MD.

DLD1-TxR and U87-TxR cells were selected by continuous exposure to stepwise increasing concentrations of PTX from DLD1 and U87 cells, respectively,¹³ while NCI-H460/R cells were selected from NCI-H460 cells after DOX selective pressure.¹⁴ MDR cancer cell lines (NCI-H460/R and DLD1-TxR) and their sensitive counterparts were maintained in RPMI 1640 medium supplemented with 10% FBS, 2mM L-glutamine, and 10,000 U/ml penicillin, 10mg/ml streptomycin, 25 µg/ml amphotericin B solutions at 37 °C in a humidified 5% CO₂ atmosphere. U87 and U87-TxR cells were grown in MEM with 10% FBS, 2 mM L-glutamine and 5000 U/ml penicillin, 5 mg/ml streptomycin solution at 37 °C in a humidified 5% CO₂ atmosphere. All cell lines were sub-cultured at 72 h intervals using 0.25% trypsin/EDTA and seeded into a fresh medium at the following densities: 8 000 cells/cm² for DLD1, DLD1-TxR, NCI-H460 and NCI-H460/R and 16 000 cells/cm² for U87 and U87-TxR.

Sulforhodamine (SRB) assay

Cell viability was assessed by SRB assay. Cells grown in 25 cm² tissue flasks were trypsinized, seeded into flat-bottomed 96-well tissue culture plates (2 000 cell/well for DLD1, DLD1-TxR, NCI-H460 and NCI-H460/R, 4 000 cell/well for U87 and U87-TxR) and incubated overnight. Treatments of colorectal carcinoma and lung carcinoma cells with **4**, **5**, **6** and **7** (0.5 - 10 µM), as well as glioblastoma cells (1 - 20 µM) lasted 48 h. After incubation period, cells were fixed in 50% trichloroacetic acid for 1 h at 4°C, rinsed in tap water and stained with 0.4% SRB in 1% acetic acid for 30 min at room temperature. Afterwards, the cells were rinsed three times in 1% acetic acid to remove the unbound stain. The protein-bound stain was extracted with solution of 10 mM Tris base. The optical density was read at λ = 540 nm with correction at λ = 670 nm in a LKB 5060-006 Microplate Reader (Vienna, Austria). IC₅₀ values were defined as the concentration of the drug that inhibited cell growth by 50% and calculated by nonlinear regression analysis using GraphPad Prism 6.

ROS and RNS production

Flow cytometric analysis upon DHE and DHR fluorescence activation was used to detect ROS levels in sensitive and MDR cancer cells. Levels of superoxide anion that activates DHE fluorescence as well as hydrogen peroxide and peroxyxynitrite anion that activate DHR fluorescence were assessed.^{39, 40} DLD1 and DLD1-TxR cells were plated and incubated overnight in 6-well plates at density of 30 000 cells/well, while U87 and U87-TxR cells were seeded at density of 200 000 cells/well. Colorectal carcinoma cells were treated with 6 µM of **6** and **7**, while glioblastoma cells were treated with 12 µM of **6** and **7**. After 48 h, adherent cells were harvested by trypsinization and incubated in medium with 1 µM DHE or DHR for 30 min at 37 °C in the dark. Cells were subsequently washed twice in PBS. DHE and DHR fluorescence was assessed in FL2 red channel and FL1 green channel, respectively. A

minimum of 10 000 events was assayed for each sample. The samples were analyzed on CyFlow Space flow cytometer (Partec, Münster, Germany).

Mitochondrial transmembrane potential detection

JC-1 is a cationic dye which accumulation in mitochondria is dependent on the mitochondrial membrane potential. Under normal conditions, JC-1 accumulates in healthy mitochondria as red aggregates detectable in FL2 channel of flow cytometer, while in depolarized mitochondria, the dye remains in the cytoplasm in monomeric form detectable in FL1 channel as green fluorescence. Thus, in mitochondria undergoing a transition from polarized to depolarized $\Delta\Psi_m$, JC-1 leaks out of the mitochondria into the cytoplasm resulting in an increase in green fluorescence and a decrease in red fluorescence.⁴¹ DLD1 and DLD1-TxR as well as U87 and U87-TxR cells were incubated overnight in 6-well plates, and then treated for 48 h with 6 μM and 12 μM of **6** and **7**, respectively. According to the manufacturer's instructions, cells were incubated with a JC-1 reagent for 15 min at 37 °C in CO₂ incubator. After two washings in 1 x Assay Buffer, the cells were re-suspended in PBS prior to flow cytometric analysis. Both red and green fluorescence emissions were detected and their ratio was analysed on a CyFlow Space flow cytometer (excitation λ = 488 nm, emission λ = 530 nm for FL1 channel and 585 nm for FL2 channel).

Cell death analysis

The percentages of apoptotic, necrotic and viable cells were determined by AV/PI labelling. All cell lines were seeded in adherent 6-well plates (30 000 cells/well for DLD1 and DLD1-TxR, 200 000 cell/well for U87 and U87-TxR) and incubated overnight. Then, DLD1 and DLD1-TxR cells were subjected to 6 μM of **6** and **7**, while U87 and U87-TxR cells were treated with 12 μM of **6** and **7**. After 48 h, total (attached and floating) cells were collected. The cells pellet was re-suspended in 100 μl of binding buffer containing AV and PI in ratio 1:1 (v/v). After the incubation period (10 min at room temperature in dark), additional 400 μl of binding buffer was added and AV/PI staining was analysed within 1 h by flow cytometry. The fluorescence intensity was measured in green FL1 and red FL2 channel on CyFlow Space flow cytometer (Partec, Münster, Germany). In each sample, 10 000 cells were recorded, and the percentages of viable (AV- PI-), early apoptotic (AV+ PI-), late apoptotic (AV+ PI+), and necrotic (AV- PI+) cells were analysed.

Assessment of autophagy markers by flow cytometry

The levels of key proteins (LC3 and p62) involved in autophagy process were detected by flow cytometry. Fluorescence intensity of rabbit anti-LC3 antibody and rabbit anti-p62 antibody both coupled with secondary Alexa Fluor 488 goat anti-rabbit IgG (H+L) antibody was measured. All cell lines were grown overnight in 6-well plates, and then colorectal carcinoma cells were exposed to 6 μM of **6** and **7**, while glioblastoma cells were treated with 12 μM of **6** and **7**. Autophagy inhibitor chloroquine (CQ), at concentration of 50 μM , was used as a positive control. After 48 h, adherent cells were harvested by trypsinization, washed twice in PBS and fixed in 4% paraformaldehyde for 10 min at room temperature. Cells were then permeabilized by adding ice-cold 90% methanol and stored for 30 min at -20 °C. After washing in PBS, cells were blocked for 60 min with 0.5% bovine serum albumin in PBS. Cells were then re-suspended in 100 μl of primary antibody diluted in 0.5% bovine serum albumin (1:1000) and incubated 60 min at room temperature. After washing in PBS, cells were

re-suspended in 100 µl of secondary antibody (1:1000) and incubated for 30 min at room temperature. Cells were subsequently washed and re-suspended in 1 ml of PBS. The fluorescence intensity was measured at FL1 channel on CyFlow Space flow cytometer (Partec, Münster, Germany).

Fluorescence microscopy

In order to visualize the formation of autophagosomes, MDR cells and their sensitive counterparts were labelled with rabbit anti-LC3 antibody coupled with secondary Alexa Fluor 488 goat anti-rabbit IgG (H+L) antibody. DLD1, DLD1-TxR, U87 and U87-TxR cells were incubated overnight in 4-chamber slides and then treated with **6**, **7** and CQ for 48 h. Afterwards, cells were washed with PBS, fixed in 4% paraformaldehyde and blocked for 60 min with 2% bovine serum albumin (Serva, Heidelberg, Germany) in 0.3% Triton™ X-100 (Merck KGaA, Darmstadt, Germany) in PBS. Rabbit anti-LC3 antibody was applied at 1:1000 dilution in PBS/0.3% Triton X-100 and cells were incubated overnight at 4°C. After washing with PBS, secondary antibody Alexa Fluor 488 goat anti-rabbit IgG (H+L) was applied at 1:1000 dilution in PBS/0.3% Triton X-100 for 120 min at room temperature. Nuclei were counterstained with Hoechst 33342 for 15 min at room temperature and cells were mounted in Mowiol (Sigma-Aldrich Chemie GmbH). The cells were visualized under the Zeiss Axiovert inverted fluorescent microscope (Carl Zeiss Foundation, Oberkochen, Germany) equipped with AxioVision4.8 software.

Combination effect analysis

The combined effects of **6** and **7** with PTX were studied on colorectal carcinoma and glioblastoma MDR cancer cells by SRB assay as previously described. In simultaneous treatments that lasted 72 h, three concentrations of **6** (0.25, 0.5 and 1 µM) and **7** (0.5, 1, and 2.5 µM) were combined with PTX (0.1 - 2.5 µM). The nature of the interaction between **6** and **7** with PTX was analysed using CalcuSyn software that uses the combination index (CI) method,⁴² based on the multiple drug effect equation. At least three data points were used for each single drug in each designed experiment. The non-constant ratio combination was chosen to assess the effect of both drugs in combination. The results are presented by fraction-affected CI graph. Values of CI < 1 point to strong additive effect referred to as synergism (the smaller value, the greater the degree of synergy). A value of CI = 1 indicates an additive effect, while values of CI > 1 point to an antagonistic effect.

Statistical analysis

Statistical analysis for flow-cytometric data was performed by two-way ANOVA test (GraphPad Prism 6 software) using Dunnett's multiple comparisons test. Statistical significance was accepted if $p < 0.05$.

Conclusions

Our results indicate that increased ROS production is essential for the mitochondrial damage induced by ferrocene-quinidine epimers additionally contributing to their selectivity towards MDR cancer cells with low antioxidant capacity. This is further confirmed by cell death analysis which showed increased capability of ferrocene-quinidine epimers to induce apoptosis and necrosis in MDR cancer cells. We

also revealed that inhibition of autophagy could represent the mechanism through which these compounds exert anticancer effect. Importantly, we showed the potential of new ferrocene-quinidine epimers to sensitize MDR cancer cells to PTX. This finding is significant due to limited options for the efficient treatment of MDR cancers. Hence, the ferrocene-quinidine epimers should be considered as new MDR selective compounds that also possess potential to reverse resistance caused by classic chemotherapeutics, such as PTX.

Acknowledgements

This research was supported by the Ministry of Education, Science and Technological Development of the Republic of Serbia (Grant No III41031) and by a grant from the Hungarian National Research Fund (OTKA K104385). This work was performed within the framework of COST Actions CM1106 (Chemical Approaches to Targeting Drug Resistance in Cancer Stem Cells) and CM1407 (Challenging organic syntheses inspired by nature - from natural products chemistry to drug discovery).

References

1. S. Kachalaki, M. Ebrahimi, L. Mohamed Khosroshahi, S. Mohammadinejad and B. Baradaran, Cancer chemoresistance; biochemical and molecular aspects: a brief overview, *European journal of pharmaceutical sciences : official journal of the European Federation for Pharmaceutical Sciences*, 2016, **89**, 20-30.
2. R. C. Todd and S. J. Lippard, Inhibition of transcription by platinum antitumor compounds, *Metallomics : integrated biometal science*, 2009, **1**, 280-291.
3. L. Kelland, The resurgence of platinum-based cancer chemotherapy, *Nature reviews. Cancer*, 2007, **7**, 573-584.
4. C. Ornelas, Application of ferrocene and its derivatives in cancer research, *New Journal of Chemistry*, 2011, **35**, 1973-1985.
5. S. S. Braga and A. M. S. Silva, A New Age for Iron: Antitumoral Ferrocenes, *Organometallics*, 2013, **32**, 5626-5639.
6. A. Ferle-Vidovic, M. Poljak-Blazi, V. Rapic and D. Skare, Ferrocenes (F168, F169) and ferrosorbitol-citrate (FSC): potential anticancer drugs, *Cancer biotherapy & radiopharmaceuticals*, 2000, **15**, 617-624.
7. J. R. Kim, K. Lee, W. T. Jung, O. J. Lee, T. H. Kim, H. J. Kim, J. S. Lee and D. J. Passaro, Validity of serum pepsinogen levels and quininium resin test combined for gastric cancer screening, *Cancer detection and prevention*, 2005, **29**, 570-575.
8. C. W. Taylor, W. S. Dalton, K. Mosley, R. T. Dorr and S. E. Salmon, Combination chemotherapy with cyclophosphamide, vincristine, adriamycin, and dexamethasone (CVAD) plus oral quinine and verapamil in patients with advanced breast cancer, *Breast cancer research and treatment*, 1997, **42**, 7-14.

9. D. Baraniak, K. Kacprzak and L. Celewicz, Synthesis of 3'-azido-3'-deoxythymidine (AZT)--Cinchona alkaloid conjugates via click chemistry: Toward novel fluorescent markers and cytostatic agents, *Bioorganic & medicinal chemistry letters*, 2011, **21**, 723-726.
10. B. I. Karolyi, S. Bosze, E. Orban, P. Sohar, L. Drahos, E. Gal and A. Csampai, Acylated mono-, bis- and tris- cinchona-based amines containing ferrocene or organic residues: synthesis, structure and in vitro antitumor activity on selected human cancer cell lines, *Molecules (Basel, Switzerland)*, 2012, **17**, 2316-2329.
11. I. Skiera, M. Antoszczak, J. Trynda, J. Wietrzyk, P. Boratynski, K. Kacprzak and A. Huczynski, Antiproliferative Activity of Polyether Antibiotic--Cinchona Alkaloid Conjugates Obtained via Click Chemistry, *Chemical biology & drug design*, 2015, **86**, 911-917.
12. L. Kocsis, I. Szabo, S. Bosze, T. Jernei, F. Hudecz and A. Csampai, Synthesis, structure and in vitro cytostatic activity of ferrocene-Cinchona hybrids, *Bioorganic & medicinal chemistry letters*, 2016, **26**, 946-949.
13. A. Podolski-Renic, T. Anđelković, J. Banković, N. Tanić, S. Ruzdijić and M. Pešić, The role of paclitaxel in the development and treatment of multidrug resistant cancer cell lines, *Biomedicine & pharmacotherapy = Biomedecine & pharmacotherapie*, 2011, **65**, 345-353.
14. M. Pešić, J. Z. Marković, D. Janković, S. Kanazir, I. D. Marković, L. Rakić and S. Ruzdijić, Induced resistance in the human non small cell lung carcinoma (NCI-H460) cell line in vitro by anticancer drugs, *Journal of chemotherapy (Florence, Italy)*, 2006, **18**, 66-73.
15. M. D. Hall, M. D. Handley and M. M. Gottesman, Is resistance useless? Multidrug resistance and collateral sensitivity, *Trends in pharmacological sciences*, 2009, **30**, 546-556.
16. K. M. Pluchino, M. D. Hall, A. S. Goldsborough, R. Callaghan and M. M. Gottesman, Collateral sensitivity as a strategy against cancer multidrug resistance, *Drug resistance updates : reviews and commentaries in antimicrobial and anticancer chemotherapy*, 2012, **15**, 98-105.
17. T. Stanković, B. Danko, A. Martins, M. Dragoj, S. Stojković, A. Isaković, H. C. Wang, Y. C. Wu, A. Hunyadi and M. Pešić, Lower antioxidative capacity of multidrug-resistant cancer cells confers collateral sensitivity to protoflavone derivatives, *Cancer chemotherapy and pharmacology*, 2015, **76**, 555-565.
18. G. Gasser, I. Ott and N. Metzler-Nolte, Organometallic anticancer compounds, *Journal of medicinal chemistry*, 2011, **54**, 3-25.
19. D. Plazuk, A. Vessieres, E. A. Hillard, O. Buriez, E. Labbe, P. Pigeon, M. A. Plamont, C. Amatore, J. Zakrzewski and G. Jaouen, A [3]ferrocenophane polyphenol showing a remarkable antiproliferative activity on breast and prostate cancer cell lines, *Journal of medicinal chemistry*, 2009, **52**, 4964-4967.
20. G. Jaouen, A. Vessieres and S. Top, Ferrocifen type anti cancer drugs, *Chemical Society reviews*, 2015, **44**, 8802-8817.
21. J. F. Arambula, R. McCall, K. J. Sidoran, D. Magda, N. A. Mitchell, C. W. Bielawski, V. M. Lynch, J. L. Sessler and K. Arumugam, Targeting Antioxidant Pathways with Ferrocenylated N-Heterocyclic Carbene Supported Gold(I) Complexes in A549 Lung Cancer Cells, *Chemical science*, 2016, **7**, 1245-1256.
22. A. Mooney, R. Tiedt, T. Maghoub, N. O'Donovan, J. Crown, B. White and P. T. Kenny, Structure--activity relationship and mode of action of N-(6-ferrocenyl-2-naphthoyl) dipeptide ethyl esters: novel organometallic anticancer compounds, *Journal of medicinal chemistry*, 2012, **55**, 5455-5466.

23. D. Krzyzanowski, G. Bartosz and A. Grzelak, Collateral sensitivity: ABCG2-overexpressing cells are more vulnerable to oxidative stress, *Free radical biology & medicine*, 2014, **76**, 47-52.
24. S. Marchi, C. Giorgi, J. M. Suski, C. Agnoletto, A. Bononi, M. Bonora, E. De Marchi, S. Missiroli, S. Patergnani, F. Poletti, A. Rimessi, J. Duszynski, M. R. Wieckowski and P. Pinton, Mitochondria-ros crosstalk in the control of cell death and aging, *Journal of signal transduction*, 2012, **2012**, 329635.
25. Y. M. Choi, H. K. Kim, W. Shim, M. A. Anwar, J. W. Kwon, H. K. Kwon, H. J. Kim, H. Jeong, H. M. Kim, D. Hwang, H. S. Kim and S. Choi, Mechanism of Cisplatin-Induced Cytotoxicity Is Correlated to Impaired Metabolism Due to Mitochondrial ROS Generation, *PLoS one*, 2015, **10**, e0135083.
26. V. Nikolettou, M. Markaki, K. Palikaras and N. Tavernarakis, Crosstalk between apoptosis, necrosis and autophagy, *Biochimica et biophysica acta*, 2013, **1833**, 3448-3459.
27. M. Valko, C. J. Rhodes, J. Moncol, M. Izakovic and M. Mazur, Free radicals, metals and antioxidants in oxidative stress-induced cancer, *Chemico-biological interactions*, 2006, **160**, 1-40.
28. R. A. Gottlieb, Mitochondria: execution central, *FEBS letters*, 2000, **482**, 6-12.
29. E. Gottlieb, S. M. Armour, M. H. Harris and C. B. Thompson, Mitochondrial membrane potential regulates matrix configuration and cytochrome c release during apoptosis, *Cell death and differentiation*, 2003, **10**, 709-717.
30. B. Levine and G. Kroemer, Autophagy in the pathogenesis of disease, *Cell*, 2008, **132**, 27-42.
31. A. Merenlender-Wagner, A. Malishkevich, Z. Shemer, M. Udawela, A. Gibbons, E. Scarr, B. Dean, J. Levine, G. Agam and I. Gozes, Autophagy has a key role in the pathophysiology of schizophrenia, *Molecular psychiatry*, 2015, **20**, 126-132.
32. Z. J. Yang, C. E. Chee, S. Huang and F. A. Sinicrope, The role of autophagy in cancer: therapeutic implications, *Molecular cancer therapeutics*, 2011, **10**, 1533-1541.
33. N. Mizushima and T. Hara, Intracellular quality control by autophagy: how does autophagy prevent neurodegeneration?, *Autophagy*, 2006, **2**, 302-304.
34. S. Pankiv, T. H. Clausen, T. Lamark, A. Brech, J. A. Bruun, H. Outzen, A. Overvatn, G. Bjorkoy and T. Johansen, p62/SQSTM1 binds directly to Atg8/LC3 to facilitate degradation of ubiquitinated protein aggregates by autophagy, *The Journal of biological chemistry*, 2007, **282**, 24131-24145.
35. G. Kroemer, G. Marino and B. Levine, Autophagy and the integrated stress response, *Molecular cell*, 2010, **40**, 280-293.
36. Y. B. Zhang, J. L. Gong, T. Y. Xing, S. P. Zheng and W. Ding, Autophagy protein p62/SQSTM1 is involved in HAMLET-induced cell death by modulating apoptosis in U87MG cells, *Cell death & disease*, 2013, **4**, e550.
37. L. Poillet-Perez, G. Despouy, R. Delage-Mourroux and M. Boyer-Guittaut, Interplay between ROS and autophagy in cancer cells, from tumor initiation to cancer therapy, *Redox biology*, 2015, **4**, 184-192.
38. Y. Ci, K. Shi, J. An, Y. Yang, K. Hui, P. Wu, L. Shi and C. Xu, ROS inhibit autophagy by downregulating ULK1 mediated by the phosphorylation of p53 in selenite-treated NB4 cells, *Cell death & disease*, 2014, **5**, e1542.
39. H. Zhao, S. Kalivendi, H. Zhang, J. Joseph, K. Nithipatikom, J. Vasquez-Vivar and B. Kalyanaraman, Superoxide reacts with hydroethidine but forms a fluorescent product that is

- distinctly different from ethidium: potential implications in intracellular fluorescence detection of superoxide, *Free radical biology & medicine*, 2003, **34**, 1359-1368.
40. D. Jourdeuil, F. L. Jourdeuil, P. S. Kutchukian, R. A. Musah, D. A. Wink and M. B. Grisham, Reaction of superoxide and nitric oxide with peroxynitrite. Implications for peroxynitrite-mediated oxidation reactions in vivo, *The Journal of biological chemistry*, 2001, **276**, 28799-28805.
 41. T. K. Garg and J. Y. Chang, 15-deoxy-delta 12, 14-Prostaglandin J2 prevents reactive oxygen species generation and mitochondrial membrane depolarization induced by oxidative stress, *BMC pharmacology*, 2004, **4**, 6.
 42. T. C. Chou and P. Talalay, Quantitative analysis of dose-effect relationships: the combined effects of multiple drugs or enzyme inhibitors, *Advances in enzyme regulation*, 1984, **22**, 27-55.